Journal of
Mechanics of
Materials and Structures

3D PHASE-EVOLUTION-BASED THERMOMECHANICAL CONSTITUTIVE MODEL OF SHAPE MEMORY POLYMER WITH FINITE ELEMENT IMPLEMENTATION

Yunxin Li, Ruoxuan Liu, Zishun Liu and Somsak Swaddiwudhipong

Volume 15, No. 3 May 2020

msp

JOURNAL OF MECHANICS OF MATERIALS AND STRUCTURES
Vol. 15, No. 3, 2020
https://doi.org/10.2140/jomms.2020.15.291

3D PHASE-EVOLUTION-BASED THERMOMECHANICAL CONSTITUTIVE MODEL OF SHAPE MEMORY POLYMER WITH FINITE ELEMENT IMPLEMENTATION

YUNXIN LI, RUOXUAN LIU, ZISHUN LIU AND SOMSAK SWADDIWUDHIPONG

Shape memory polymers (SMPs) are a class of smart materials which can undergo transition between two different states (temporary shape and permanent state) induced by external stimuli, such as temperature, light etc. In order to study the deformation behavior of this fast-developing SMP structures, the key points are formulating suitable theoretical constitutive models to correctly reflect the material behavior and developing appropriate numerical simulation techniques to handle complex structures. In this paper, we proposed a three-dimensional (3D) thermomechanical constitutive model of SMPs and its implementation as a user material subroutine, UMAT, in a finite element package ABAQUS. The shape memory effects of the SMPs under three different loading patterns are simulated by the proposed approach and the acquired numerical results are compared with theoretical computational results and available experimental data. They agree reasonably well. Two SMP structural examples are presented to demonstrate the feasibility of the proposed approach. The exercises involve the analyses of (i) an intelligent hexachiral deployable structure and (ii) a 3D self-folding structure achieved through a 2D plate.

1. Introduction

Shape memory polymers (SMPs) are soft and intelligent materials that can recover their permanent configuration from a temporary deformed shape upon the application of stimuli, such as, temperature, water, light and electricity [Li et al. 2015; Zheng et al. 2018; Conti et al. 2007; Huang et al. 2005; Lendlein et al. 2005; Qi and Dunn 2010]. SMPs have several advantages over the traditional shape memory materials (*e.g.* shape memory alloys) as SMPs are biodegradable, biocompatible, light weight, low cost and able to render large deformation [Baghani et al. 2012; Hager et al. 2015; Leng et al. 2009] and hence SMPs have great potential applications in various fields, such as, aerospace structures [Behl et al. 2010; Hu et al. 2012], functional textiles [Castano and Flatau 2014; Hu and Chen 2010], biomedicine [Lendlein et al. 2010; Yakacki and Gall 2009; Liu et al. 2019b], self-healing materials [Luo and Mather 2013; Shojaei and Li 2014; Shojaei et al. 2013] and pattern transformations [He et al. 2015; Liu et al. 2015].

The diverse applications and benefits of SMPs in various fields, especially those of critical importance, have stimulated a great progress in theoretical [Pan et al. 2018], numerical [Pan et al. 2019; Li et al. 2018; Eskandari et al. 2018; Valizadeh et al. 2018] and experimental studies [Liu et al. 2019a] of these materials on their deformation mechanism. The experimental approach is essential but normally costly and time

Zishun Liu is the corresponding author.
Keywords: shape memory polymer, constitutive model, finite element method.

consuming. On the contrary, once the material parameters are evaluated from test data, the theoretical and numerical studies provide comprehensive descriptions and predictions of the mechanical behavior of SMPs with substantially less cost and time. The theory describing SMPs dated back more than two decades ago [Huang et al. 2020]. Tobushi et al. [1997] recommended a viscoelastic modeling approach for SMPs in 1997. They developed a one-dimensional rheological model that qualitatively describes the shape memory process by introducing an irreversible slip element in traditional spring-damper system. Based on the above approach, Lin and Chen [1999] proposed another viscoelastic model to predict the shape memory effect and rate-dependent behavior of polyurethanes. Diani et al. [2006] explored a three-dimensional (3D) viscoelastic constitutive model that was thermodynamically motivated. Though the model is able to capture some key features of shape memory behavior, it is incapable of predicting the details of response in thermodynamic cycle. To cater for the time-dependent and temperature-dependent characteristics of the amorphous SMPs, Nguyen et al. [2008] developed a thermo-viscoelastic constitutive model which considered structural and stress relaxation as the primary molecular mechanisms of the shape memory effect and its time-dependency. Srivastava et al. [2010] established a thermo-mechanically coupled large-deformation constitutive model and determined the model parameters using stress-strain experimental data. The model is able to predict the shape memory behavior of the SMPs with satisfactory results. Yu et al. [2014] introduced a 3D viscoelastic model which combined a spring element and several Maxwell elements in parallel fashion to represent different active relaxation mechanisms in SMPs. Based on multiplicative decompositions of the deformation gradient, Li et al. [2017a] proposed a novel viscoelastic constitutive model for SMPs. To reduce the parameters of describing SMP constitutive model, the fractional order models are proposed. Fang et al. [2018] developed a multi-branch thermoviscoelastic model which was valid for multi-shape memory effect of SMP by introducing the shift factor. Pan and Liu [2018] presented a new fractional viscoelastic constitutive model for SMPs to describe the phase transition phenomenon of SMPs with various constitutive components defined around the glass transition temperature. All these two models reduced considerably the number of material parameters required to describe the phase transition phenomenon of SMPs. The phenomenological phase transition modeling of SMPs was introduced in [Liu et al. 2006], which considered SMPs as a mixture of different phases that are interchangeable depending on the heat stimulus. Based on that work, many comprehensive phenomenological models of SMPs were formulated and presented in [Baghani et al. 2014; Chen and Lagoudas 2008a; Chen and Lagoudas 2008b; Gilormini and Diani 2012; Gu et al. 2015; Li et al. 2017b; Li and Liu 2018; Moon et al. 2015; Qi et al. 2008; Volk et al. 2010; Yang and Li 2015].

Numerical approach has also been applied to study the thermomechanical behavior of SMPs. Qi et al. [2008] implemented a 3D model into ABAQUS user material subroutine (UMAT) for amorphous SMPs. Reese et al. [2010] formulated a new model in a micromechanical as well as a macro-mechanical format and implemented this model into software "FEAP" (a finite element analysis program originated by researchers at the University of California, Berkeley). The generalized Maxwell model and WLF equation which are available in ABAQUS were adopted by Diani et al. [2012] to model SMP materials. Baghani et al. [2012] employed the finite element method (FEM) for SMPs to study 3D shape memory beams and medical stents while Tian and Venkatesh [2013] implemented the FEM for indentation of SMPs. The FEM was also adopted by Li et al. [2015] to conduct the thermomechanical behavior analysis of polyurethane. Recently, Pieczyska et al. [2017] developed the FEM in AceGen/AceFEM environment to simulate the cyclic tensile tests of SMPs.

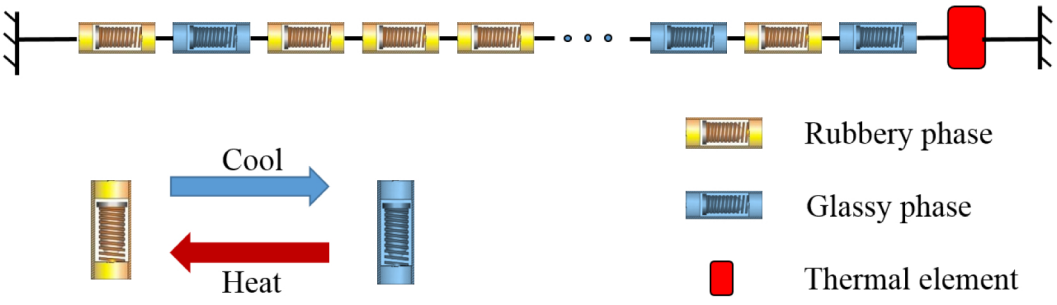

Figure 1. Schematic illustration of phase-evolution-based thermomechanical constitutive model reflecting process of phase transition between yellow rubbery phase and glassy phase in pewter.

In 2017, we introduced a phase-evolution-based thermomechanical constitutive model which can capture the shape memory effect of amorphous SMPs [2017b]. However, the model is of just a one-dimensional (1D) framework and hence is not able to trace and evaluate the deformation behavior of complex SMP structures. The present article extends the 1D SMP constitutive model into a 3D platform with an implementation as a UMAT subroutine in the finite element package ABAQUS. This enables us to apply the proposed constitutive model to simulate the deformation behavior of any complex SMP structures effectively and conveniently.

The paper is organized as follows. In Section 2, we re-introduce briefly a 1D phase-evolution-based thermomechanical constitutive model for SMPs. The 1D constitutive model is extended to a 3D form and then implemented in ABAQUS in Section 3. The detailed formulations and procedural considerations associated with FEM are provided in this section. Section 4 involves the verifications of both theoretical considerations and numerical implementation through the comparison of numerical solutions with theoretical computational results and available experimental data. Reasonably good agreement is observed. The proposed 3D constitutive model for SMPs with FEM implementation is applied to analyze two complex SMP structures and the outcomes are reported in Section 5. Finally, the concluding remarks are given in Section 6.

2. Constitutive model for SMPs

Prior to the presentation of a 3D phase-evolution-based thermomechanical constitutive model formulation in Section 3, a 1D development that has been elaborated earlier by Li et al. [2017b] is briefly described in this section.

2.1. ***General description of the constitutive model.*** In this approach, SMPs are considered as a mixture of the yellow rubbery phase regions and the glassy phase regions in pewter color as shown in Figure 1. The volume fraction of each of the former is $\Delta\gamma_r^j$ and the latter as $\Delta\gamma_g^j$, where the total sum is unity, i.e., $\Sigma\Delta\gamma_g^j + \Sigma\Delta\gamma_r^j = 1$. The total strain of the adopted model including that of thermal effect is expressed as

$$\varepsilon_{\text{total}} = \Sigma\Delta\gamma_r^j\varepsilon_{\text{rubbery}}^j + \Sigma\Delta\gamma_g^j\varepsilon_{\text{glassy}}^j + \varepsilon_T \tag{1}$$

where ε_T is the thermal strain, $\varepsilon^j_{\text{rubbery}}$ and $\varepsilon^j_{\text{glassy}}$ are strains in any j-th rubbery and any j-th glassy phase regions, respectively.

These two kinds of springs which represent two different phases (yellow for rubbery phase and pewter for glassy phase) are interchangeable governed by the variation of temperature. As the temperature decreases, certain rubbery phase regions will be transformed into those of the glassy phase where part of their deformations are frozen. In the newly formed glassy phase regions, the frozen strain and residual mechanical strain are denoted by $\varepsilon_{\text{frozen}}$ and $\varepsilon_{g\text{-mechanics}}$, respectively. Li et al. [2017b] defined the frozen strain $\varepsilon_{\text{frozen}}$ as

$$\varepsilon_{\text{frozen}} = \varepsilon_{r\text{-mechanics}} - f(T)\varepsilon_{r\text{-mechanics}} \tag{2}$$

where $\varepsilon_{r\text{-mechanics}}$ is the mechanical strain in the corresponding previous rubbery phase regions. $f(T)$ is the ratio of the mechanical strains corresponding to the two transformed phase regions, i.e., $f(T) = \varepsilon_{g\text{-mechanics}}/\varepsilon_{r\text{-mechanics}}$. $f(T)$ is calibrated based on experimental data.

At the increase in temperature, the transition glassy phase regions are reverted back to those of the rubbery phase while the frozen strain is released, leaving only the mechanical strain $\varepsilon_{r\text{-mechanics}}$ in the rubbery phase regions. The strains in the glassy phase regions comprise both the mechanical strain $\varepsilon_{g\text{-mechanics}}$ and the frozen strain $\varepsilon_{\text{frozen}}$. Hence, the total strain in Eq. (1) at the latter stage can be written as

$$\varepsilon_{\text{total}} = \Sigma\Delta\gamma_r^j \varepsilon^j_{r\text{-mechanics}} + \Sigma\Delta\gamma_g^j \left(\varepsilon^j_{g\text{-mechanics}} + \varepsilon^j_{\text{frozen}}\right) + \varepsilon_T \tag{3}$$

The stress in each phase region is described by Hooke's law as stipulated in Eqs. (4) and (5):

$$\sigma_r^j = E_r \varepsilon^j_{r\text{-mechanics}}, \tag{4}$$

$$\sigma_g^j = E_g \varepsilon^j_{g\text{-mechanics}}, \tag{5}$$

where E_r and E_g are the Young's moduli of the rubbery and glassy phase regions, respectively.

All spring elements shown in Figure 1 are in series and hence the stress in any phase region is the same and equals the total stress, namely,

$$\sigma_{\text{total}} = \sigma_r^j = \sigma_g^j \tag{6}$$

As the mechanical strain of any j-th rubbery phase region remains unchanged, we have $\varepsilon^j_{r\text{-mechanics}} = \varepsilon_{r\text{-mechanics}}$. This is similarly true for the mechanical strain of any j-th glassy phase region and hence we also have $\varepsilon^j_{g\text{-mechanics}} = \varepsilon_{g\text{-mechanics}}$. Substituting these 2 identities into Eq. (3), the total strain becomes

$$\varepsilon_{\text{total}} = (1-\gamma)\varepsilon_{r\text{-mechanics}} + \gamma\varepsilon_{g\text{-mechanics}} + \varepsilon_f + \varepsilon_T \tag{7}$$

In Eq. (7), $\gamma = \Sigma\Delta\gamma_g^j$ denotes the fraction of the glassy phase and hence the fraction of the rubbery phase is $1-\gamma = \Sigma\Delta\gamma_r^j$. The total frozen strain in SMPs is then represented by the expression, $\varepsilon_f = \Sigma\Delta\gamma_g^j \varepsilon^j_{\text{frozen}}$.

2.2. ***Governing equation of shape memory effect.*** An incremental approach is adopted to establish the governing equations of SMP model covering the continuous phase transition processes. During the cooling period, the temperature decreases from a high temperature T_h to a low value of T_l. The temperature interval of interest $[T_h, T_l]$ is divided into numerous small increments. For a generic advancement of

temperature $[T_{\text{cool}}^{n-1}, T_{\text{cool}}^{n}]$, the stress and strain are denoted by superscript n-1 at temperature $T_{\text{cool}}^{n-1}$and that of n at temperature T_{cool}^{n}, respectively.

When temperature drops from T_{cool}^{n-1} to T_{cool}^{n}, certain portions of the rubbery phase regions of $(\Delta\gamma^n)$ are transformed into those of the glassy phase and parts of deformations $(\varepsilon_{\text{frozen}}^{n})$ are frozen. The total frozen strain ε_f^n at T_{cool}^{n} is

$$\varepsilon_f^n = \sum_{j=1}^{n} \Delta\gamma_g^j \varepsilon_{\text{frozen}}^j = \varepsilon_f^{n-1} + \Delta\gamma^n \varepsilon_{\text{frozen}}^n \tag{8}$$

where $\varepsilon_f^{n-1} = \sum_{j=1}^{n-1} \Delta\gamma^j \varepsilon_{\text{frozen}}^j$ is the total frozen strain at temperature T_{cool}^{n-1}.

Substituting Eq. (2) into Eq. (8) yields

$$\varepsilon_f^n = \varepsilon_f^{n-1} + \Delta\gamma^n (1 - f(T)) \varepsilon_{r\text{-mechanics}}^n \,. \tag{9}$$

Here $\varepsilon_f^n - \varepsilon_f^{n-1} = \Delta\varepsilon_f^n$ is the small increment of total frozen strain. Inserting Eq. (4)–Eq. (7) into Eq. (9), we obtain the expressions for σ_{total}^n and $\Delta\varepsilon_f^n$ at T_{cool}^{n} as given by

$$\sigma_{\text{total}}^n = \frac{\varepsilon_{\text{total}}^n - \varepsilon_f^n - \varepsilon_T^n}{\dfrac{\gamma^n}{E_g} + \dfrac{1-\gamma^n}{E_r}}, \tag{10}$$

$$\Delta\varepsilon_f^n = \Delta\gamma^n [1 - f(T)] \frac{\varepsilon_{\text{total}}^{n-1} - \varepsilon_f^{n-1} - \varepsilon_T^{n-1}}{E_r\left(\dfrac{\gamma^{n-1}}{E_g} + \dfrac{1-\gamma^{n-1}}{E_r}\right)}. \tag{11}$$

Expressing Eq. (11) in differential form, the governing equations of shape memory effect can be written collectively in general form as

$$\begin{cases} \sigma_{\text{total}} = \dfrac{\varepsilon_{\text{total}} - \varepsilon_f - \varepsilon_T}{\dfrac{\gamma}{E_g} + \dfrac{1-\gamma}{E_r}}, \\ \dfrac{d\varepsilon_f}{dT} = \dfrac{d\gamma}{dT}[1 - f(T)] \dfrac{\varepsilon_{\text{total}} - \varepsilon_f - \varepsilon_T}{E_r\left(\dfrac{\gamma}{E_g} + \dfrac{1-\gamma}{E_r}\right)}. \end{cases} \tag{12}$$

2.3. ***Thermal deformation.*** The thermal strain ε_T is

$$\varepsilon_T = \int_{T_0}^{T} \alpha dT \tag{13}$$

where α is the coefficient of thermal expansion (CTE) and T_0 is the reference temperature.

3. Finite element approach

3.1. ***3D form of constitutive model.*** To apply the proposed constitutive relationship into finite element computation, the constitutive model of 1D form must be generalized into 3D form [Lucchesi et al. 2019]. Therefore, we extend the previous SMP constitutive model into a 3D form and implement the latter in a

finite element package ABAQUS through its UMAT subroutine. For a 3D isotropic solid, the total strain and the total stress can be rewritten as follows:

$$\varepsilon_{ij}^{\text{total}} = (1-\gamma)\varepsilon_{ij}^{r\text{-mechanics}} + \gamma\varepsilon_{ij}^{g\text{-mechanics}} + \varepsilon_{ij}^{f} + \varepsilon_{ij}^{T} \quad i, j = x, y, z \tag{14}$$

$$\sigma_{ij}^{\text{total}} = \sigma_{ij}^{r} = \sigma_{ij}^{g} \quad i, j = x, y, z \tag{15}$$

The one-dimensional (1D) governing equation (Eq. (4)) of the rubbery phase element can be generalized into a 3D form as shown in Eq. (16) and Eq. (17).

$$\sigma_{xx}^{r} = \lambda_r \varepsilon_V^{r\text{-mechanics}} + 2\mu_r \varepsilon_{xx}^{r\text{-mechanics}}, \quad \text{etc.} \tag{16}$$

$$\sigma_{xy}^{r} = 2\mu_r \varepsilon_{xy}^{r\text{-mechanics}}, \quad \text{etc.} \tag{17}$$

where $\varepsilon_V^{r\text{-mechanics}} = \varepsilon_{xx}^{r\text{-mechanics}} + \varepsilon_{yy}^{r\text{-mechanics}} + \varepsilon_{zz}^{r\text{-mechanics}}$, λ_r and μ_r are the Lame constants of the rubbery phase element.

Similarly, the 3D form model of the glassy phase element is expressed as

$$\sigma_{xx}^{g} = \lambda_g \varepsilon_V^{g\text{-mechanics}} + 2\mu_g \varepsilon_{xx}^{g\text{-mechanics}}, \quad \text{etc.} \tag{18}$$

$$\sigma_{xy}^{g} = 2\mu_g \varepsilon_{xy}^{g\text{-mechanics}}, \quad \text{etc.} \tag{19}$$

where $\varepsilon_V^{g\text{-mechanics}} = \varepsilon_{xx}^{g\text{-mechanics}} + \varepsilon_{yy}^{g\text{-mechanics}} + \varepsilon_{zz}^{g\text{-mechanics}}$, λ_g and μ_g are the Lame constants of the glassy phase element.

The 3D form of the thermal strain in Eq. (13) is thus

$$\varepsilon_{ij}^{T} = \delta_{ij} \int_{T_0}^{T} \alpha \, dT, \quad i, j = x, y, z \tag{20}$$

In view of Eq. (16) and Eq. (18), Eq. (15) becomes

$$\lambda_r \varepsilon_V^{r\text{-mechanics}} + 2\mu_r \varepsilon_{xx}^{r\text{-mechanics}} = \lambda_g \varepsilon_V^{g\text{-mechanics}} + 2\mu_g \varepsilon_{xx}^{g\text{-mechanics}}, \quad \text{etc.} \tag{21}$$

Eq. (14) provides the basis for the expressions of various principal components of the total strain and volume deformation $\varepsilon_V^{\text{total}} = \varepsilon_{xx}^{\text{total}} + \varepsilon_{yy}^{\text{total}} + \varepsilon_{zz}^{\text{total}}$ as given in Eq. (22) and Eq. (23).

$$\varepsilon_{xx}^{\text{total}} = (1-\gamma)\varepsilon_{xx}^{r\text{-mechanics}} + \gamma\varepsilon_{xx}^{g\text{-mechanics}} + \varepsilon_{xx}^{f} + \varepsilon_{xx}^{T}, \quad \text{etc.} \tag{22}$$

$$\varepsilon_V^{\text{total}} = (1-\gamma)\varepsilon_V^{r\text{-mechanics}} + \gamma\varepsilon_V^{g\text{-mechanics}} + \varepsilon_V^{f} + \varepsilon_V^{T}. \tag{23}$$

Inserting Eq. (22) and Eq. (23) into Eq. (21), we have

$$\varepsilon_{xx}^{g\text{-mechanics}} = \frac{\lambda_r(\varepsilon_V^{\text{total}} - \varepsilon_V^{f} - \varepsilon_V^{T}) + 2\mu_r(\varepsilon_{xx}^{\text{total}} - \varepsilon_{xx}^{f} - \varepsilon_{xx}^{T}) - (\gamma\lambda_r + (1-\gamma)\lambda_g)\varepsilon_V^{g\text{-mechanics}}}{2(\gamma\mu_r + (1-\gamma)\mu_g)}, \quad \text{etc.,} \tag{24}$$

$$\varepsilon_V^{g\text{-mechanics}} = \frac{(3\lambda_r + 2\mu_r)(\varepsilon_V^{\text{total}} - \varepsilon_V^{f} - \varepsilon_V^{T})}{3(\gamma\lambda_r + (1-\gamma)\lambda_g) + 2(\gamma\mu_r + (1-\gamma)\mu_g)}. \tag{25}$$

The shear components of total strain $\varepsilon^{g\text{-mechanics}}$ can be derived from Eq. (14) to give

$$\varepsilon_{xy}^{g\text{-mechanics}} = \frac{\left(\varepsilon_{xy}^{\text{total}} - \varepsilon_{xy}^{f} - \varepsilon_{xy}^{T}\right)\mu_r}{(1-\gamma)\mu_g + \gamma\mu_r}, \quad \text{etc.} \tag{26}$$

Substituting Eq. (24) and Eq. (26) into Eq. (18) and Eq. (19) yields the following 3D form of governing equations for the constitutive model.

$$\sigma_{xx}^{\text{total}} = \left(\varepsilon_V^{\text{total}} - \varepsilon_V^{f} - \varepsilon_V^{T}\right)\lambda(T) + 2\mu(T)\left(\varepsilon_{xx}^{\text{total}} - \varepsilon_{xx}^{f} - \varepsilon_{xx}^{T}\right), \quad \text{etc.}, \tag{27}$$

$$\sigma_{xy}^{\text{total}} = 2\mu(T)\left(\varepsilon_{xy}^{\text{total}} - \varepsilon_{xy}^{f} - \varepsilon_{xy}^{T}\right), \quad \text{etc.} \tag{28}$$

where

$$\lambda(T) = \frac{\mu_g\lambda_r}{\gamma\mu_r + (1-\gamma)\mu_g} + \frac{\gamma\mu_r\lambda_g - \gamma\mu_g\lambda_r}{\gamma\mu_r + (1-\gamma)\mu_g} * \frac{(3\lambda_r + 2\mu_r)}{3(\gamma\lambda_r + (1-\gamma)\lambda_g) + 2(\gamma\mu_r + (1-\gamma)\mu_g)},$$

$$\mu(T) = \frac{\mu_g\mu_r}{\gamma\mu_r + (1-\gamma)\mu_g}.$$

The constitutive relations in Eq. (27) and Eq. (28) can be collectively expressed as

$$\sigma_{ij} = \lambda(T)\delta_{ij}\varepsilon_{kk}^{el} + 2\mu(T)\varepsilon_{ij}^{el} \tag{29}$$

where $\varepsilon_{ij}^{el} = \varepsilon_{ij}^{\text{total}} - \varepsilon_{ij}^{f} - \varepsilon_{ij}^{T}$. Eq. (29) can be written in a Jaumann rate form as

$$\dot{\sigma}_{ij}^{J} = \lambda(T)\delta_{ij}\dot{\varepsilon}_{kk}^{el} + 2\mu(T)\dot{\varepsilon}_{ij}^{el} + \dot{\lambda}(T)\delta_{ij}\varepsilon_{kk}^{el} + 2\dot{\mu}(T)\varepsilon_{ij}^{el} \tag{30}$$

The Jaumann rate equation of Eq. (30) is integrated in a co-rotational framework to render

$$\Delta\sigma_{ij}^{J} = \lambda(T)\delta_{ij}\Delta\varepsilon_{kk}^{el} + 2\mu(T)\Delta\varepsilon_{ij}^{el} + \Delta\lambda(T)\delta_{ij}\varepsilon_{kk}^{el} + 2\Delta\mu(T)\varepsilon_{ij}^{el} \tag{31}$$

Once the frozen strain ε_{ij}^{f} is established, Eq. (31) provides us the basis for a 3D implementation of finite element model via UMAT subroutine in ABAQUS.

3.2. ***3D form of frozen strain.*** To calculate the frozen strain in Eq. (14), we have to recast the constitutive equation of shape memory effect (Eq. 12) into a three-dimensional form as shown in Eq. (32).

$$\begin{cases} \sigma_{ij}^{\text{total}} = C_{ij}\left(\varepsilon_{ij}^{\text{total}} - \varepsilon_{ij}^{f} - \varepsilon_{ij}^{T}\right) \\ \dfrac{d\varepsilon_{ij}^{f}}{dT} = \dfrac{d\gamma}{dT}[1 - f(T)]\left(C_r^{-1}\right)_{ij} C_{ij}\left(\varepsilon_{ij}^{\text{total}} - \varepsilon_{ij}^{f} - \varepsilon_{ij}^{T}\right) \end{cases} \tag{32}$$

where C_{ij} is the component of SMPs stiffness matrix C and $\left(C_r^{-1}\right)_{ij}$ represents the component of inverse stiffness matrix for any rubbery phase element. In view of Eq. (16), Eq. (17) and Eq. (29), the stiffness matrix of the rubbery phase elements (which is labeled by r) and consequently that of shape memory

material are expressed respectively as

$$\boldsymbol{C}_r = \begin{bmatrix} \lambda_r+2\mu_r & \lambda_r & \lambda_r & 0 & 0 & 0 \\ \lambda_r & \lambda_r+2\mu_r & \lambda_r & 0 & 0 & 0 \\ \lambda_r & \lambda_r & \lambda_r+2\mu_r & 0 & 0 & 0 \\ 0 & 0 & 0 & \mu_r & 0 & 0 \\ 0 & 0 & 0 & 0 & \mu_r & 0 \\ 0 & 0 & 0 & 0 & 0 & \mu_r \end{bmatrix} \tag{33}$$

$$\boldsymbol{C} = \begin{bmatrix} \lambda+2\mu & \lambda & \lambda & 0 & 0 & 0 \\ \lambda & \lambda+2\mu & \lambda & 0 & 0 & 0 \\ \lambda & \lambda & \lambda+2\mu & 0 & 0 & 0 \\ 0 & 0 & 0 & \mu & 0 & 0 \\ 0 & 0 & 0 & 0 & \mu & 0 \\ 0 & 0 & 0 & 0 & 0 & \mu \end{bmatrix} \tag{34}$$

The incremental form of the frozen strain in Eq. (32) is thus

$$\begin{cases} \Delta\varepsilon_{f\text{-}ij} = (\gamma_{ij} - \gamma_{ij}) * (1-f) * (\varepsilon_{\text{pre-}ij} - \varepsilon_{f\text{-}ij} - \varepsilon_{T\text{-}ij}) * CRC_{ij} \\ \varepsilon_{f\text{-}ij} = \varepsilon_{f\text{-}ij} + \Delta\varepsilon_{f\text{-}ij} \end{cases} \tag{35}$$

where $CRC_{ij} = (C_r^{-1})_{in}C_{nj}$. Eq. (35) provides the iterative relations for the determination of the frozen strain suitable for finite element implementation.

4. Verification of proposed numerical model

We have developed a numerical model describing the complex thermomechanical characteristics of SMPs by implementing the above 3D constitutive relations as a UMAT subroutine in the finite element package ABAQUS. The proposed model is verified through the comparisons of the numerical solutions acquired in the present study with those obtained experimentally and via the analytical approach reported earlier in [Liu et al. 2006; 2017b]. The material parameters adopted in the exercises as stipulated in Table 1

T_g	310 K
T_h	338 K
T_l	298 K
γ	$1 - \dfrac{1}{1+0.000036(T_h-T)^4}$
E_g	8538.93 MPa
N	719.28 mol/m^3
E_r	$3NkT$ MPa
α	$-2.066\times10^{-4} + 1.52\times10^{-6}T)$ K^{-1}
f	$\begin{cases} 0 & (T \le T_g) \\ (T-T_g)/T_g & (T > T_g) \end{cases}$

Table 1. Material parameters adopted from [Li et al. 2017b].

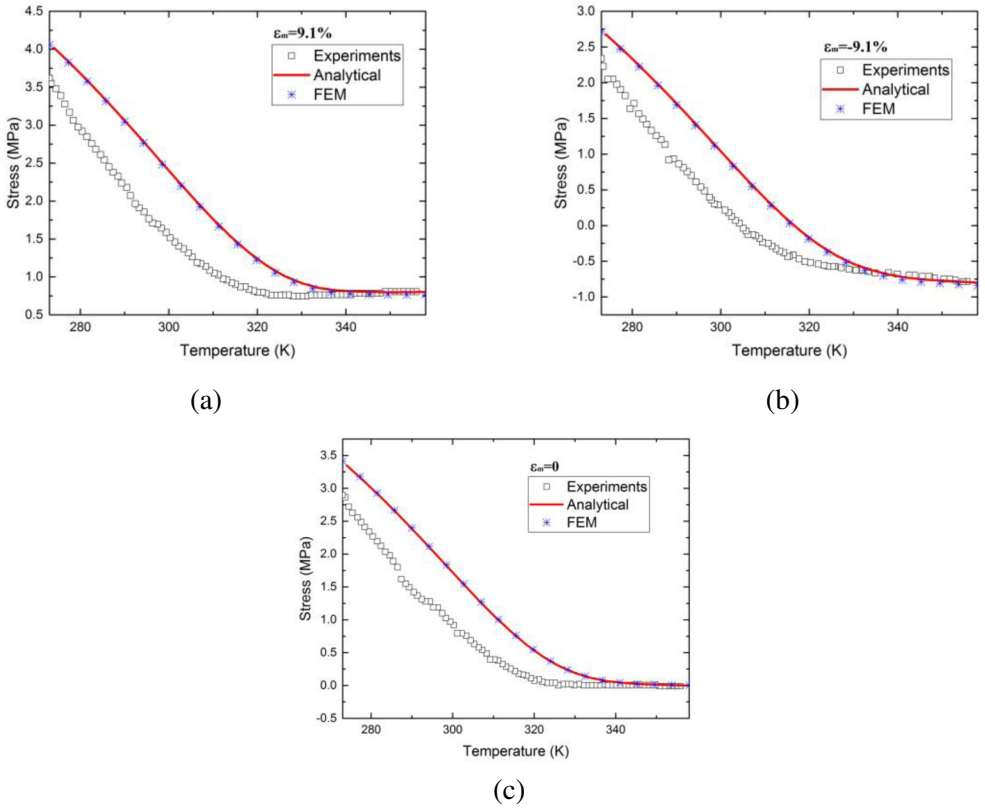

Figure 2. Comparison of FE solutions with theoretical computational results (using "analytical" symbol in figures) and experimental results [Liu et al. 2006] of stress in cooling process under various loading patterns: (a) $\varepsilon_m = 9.1\%$ (tension); (b) $\varepsilon_m = -9.1\%$ (compression); (c) $\varepsilon_m = 0$ (zero-strain).

are the same as those employed in Table 2 of [Li et al. 2017b]. The shape memory effects of this SMP material under various types of loading patterns namely those in (i) tension, (ii) compression and (iii) zero-strain condition are considered in the study.

Typically, the shape memory cycle comprises four processes. They are: (1) loading at a high temperature, (2) cooling under fixed strain constraint, (3) unloading at a low temperature and (4) reheating. The stress-temperature response in the cooling process and strain-temperature response in the reheating process are the key characteristics of the shape memory effect. Thus, we reproduce the thermomechanical behavior of SMPs during both the cooling period in Figure 2 and the reheating process in Figure 3. To demonstrate the stability of the proposed finite element approach, the numerical solutions are compared with both theoretical computational results (directly from theoretical formulas) and available experimental data. Figure 2 and Figure 3 show that the acquired numerical solutions match well with the computational results and provide similar trends with those obtained experimentally as reported by in [Liu et al. 2006].

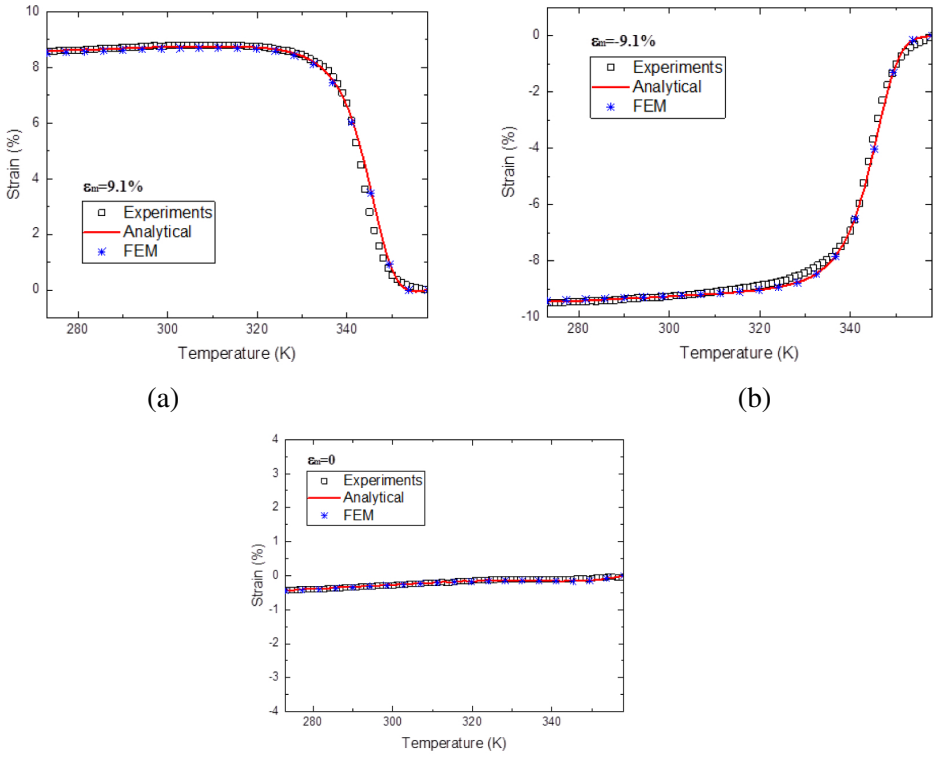

Figure 3. Comparison of FE solutions with theoretical computational results (using "analytical" symbol in figures) and experimental results [Liu et al. 2006] of strain in the reheating process under various loading patterns: (a) $\varepsilon_m = 9.1\%$ (tension); (b) $\varepsilon_m = -9.1\%$ (compression); (c) $\varepsilon_m = 0$ (zero-strain).

5. Deformation of complex structures

To further demonstrate the robustness of the present constitutive theory and its finite element implementation, the proposed numerical model is adopted to simulate the response of 2 complex SMP structures. They are: (i) a deployable structure to be presented in Section 5.1 and (ii) a self-folding structure from a 2D plate to a 3D structure to be elaborated in Section 5.2.

5.1. ***Deployable SMP structure.*** Intelligent deployable structure is a kind of mechanical components that demonstrate significant expansion in area and/or volume influenced by a control signal. It has a great potential for critical applications in various fields. A few examples include those employed as deployable antennas in the area of space exploration and intravascular stents in biomedical applications. With a unique combination of favorable properties (*e.g.,* low density and low cost), SMPs are considered as an ideal material for intelligent deployable structures. Rossiter et al. [2012] designed a SMP hexachiral deployable structure which can be kept at a compact size without any restraint and later be expanded to form a significantly larger structure after its shape recovery.

We adopt the proposed finite element model to simulate the hexachiral deployable structure depicted in Figure 4. The geometry of the structure is the same as the experimental sample used by Rossiter et al. [2012]. Figure 4(a) illustrates the SMP hexachiral structure as a full-sized deployment structure in its initial state. The SMP hexachiral structure is heated to a high temperature above T_g and then compressed to a compact configuration as depicted in Figure 4(b). It is then cooled down to retain the deformed compact shape. After removing the load constraint, an insignificant amount of elastic recovery is observed as shown in Figure 4(c). Finally, the hexachiral structure is expanded to its original full-size

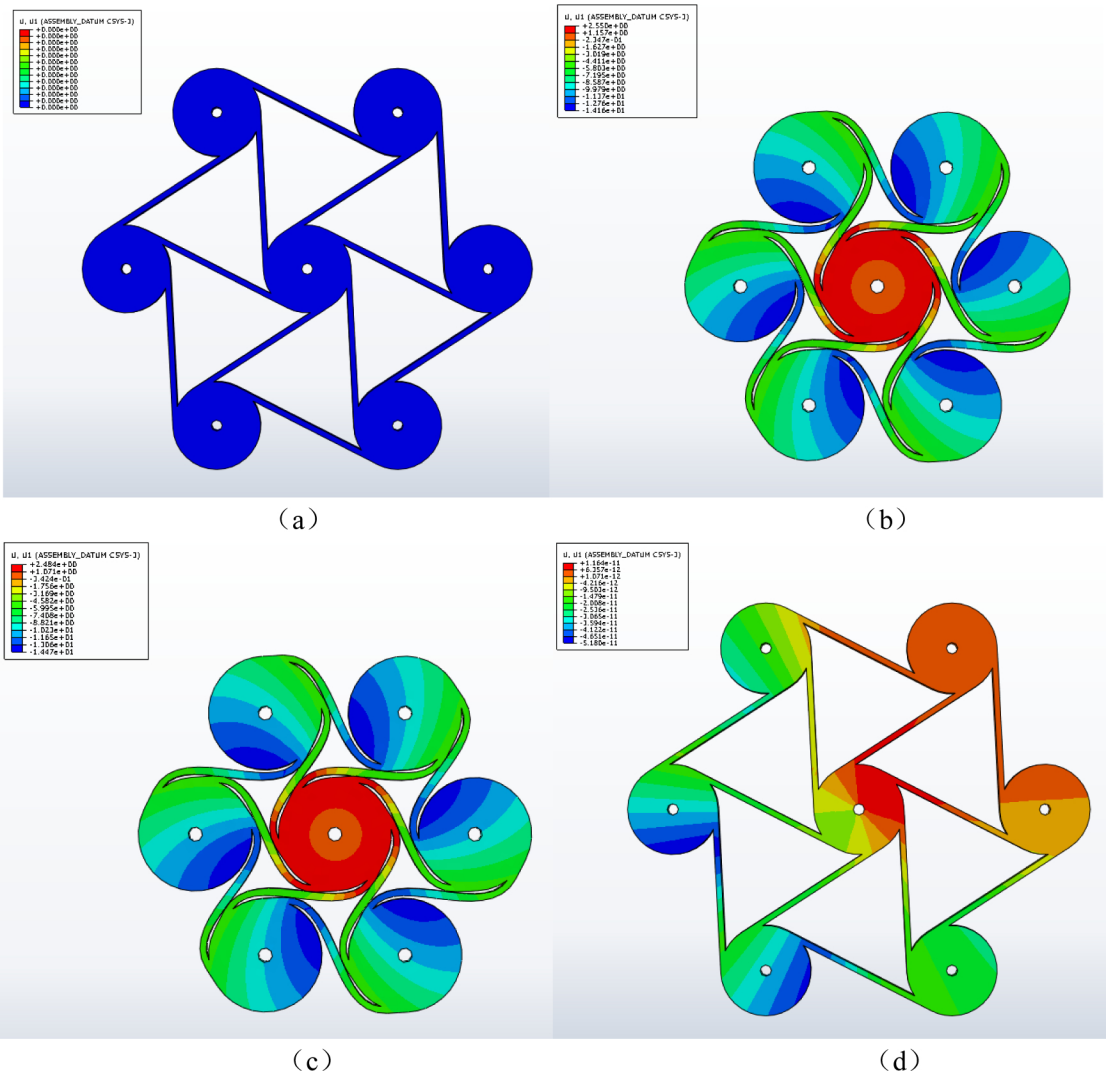

Figure 4. Finite element simulation of hexachiral deployable structure: (a) initial state; (b) compressed state at high temperature; (c) unloaded state after cooling; (d) deployed structure after shape recovery. Colors indicate radial displacements in a cylindrical coordinate system.

structure for deployment by reheating it to a high temperature as displayed in Figure 4(d). The present simulated results as illustrated in Figure 4 are consistent with the experimental outcomes observed by Rossiter et al. [2012]. This demonstrates the feasibility and stability of the proposed constitutive model to simulate various processes of development of the SMP deployable structure.

5.2. ***Self-folding structure.*** Complex three-dimensional (3D) manufacturing processes are often required in the industry. They are normally costly and time-consuming. Self-folding process provides a fast and effective technique for manufacturing three-dimensional structures. Self-folding is a common structural manufacturing method that can be observed in nature, e.g., those in organic molecules, insect wings, human brain and leaves of plants. This has great application prospects in various fields, including space exploration, logistics transportation and flexible electronic devices [Tolley et al. 2014]. The application of SMPs in self-folding structures has recently attracted wide attention. In this section, we design a self-folding structure using SMP materials and simulate the deformation processes of the self-folding structure from its two-dimensional plate strip to a three-dimensional structure.

The initial configuration of the self-folding structure is a two-dimensional rectangular plate strip shown in Figure 5. The plate thickness comprises two layers of the same shape memory polymer material. The bottom layer in dark blue covers the whole board while the upper SMPs layer is divided into several regions of blue portions connected intermittently by smaller yellow parts of self-folding hinge regions which can later be heated locally.

Figure 6 illustrates the deformation processes transforming a two-dimensional pattern to a three-dimensional configuration. First, we heat the original plate structure to a high temperature and apply a compressive deformation along the length of the plate. While retaining the deformed shape, the temperature of the whole structure is reduced to ensure that the deformation is frozen to keep the structure in the deformed configuration even after unloading. Finally, while keeping the temperature of the blue and dark blue regions constant, the yellow self-folding hinge regions are heated locally to extend the latter regions to their original shapes. As the deformation of the bottom plate restricts the expansion of the yellow

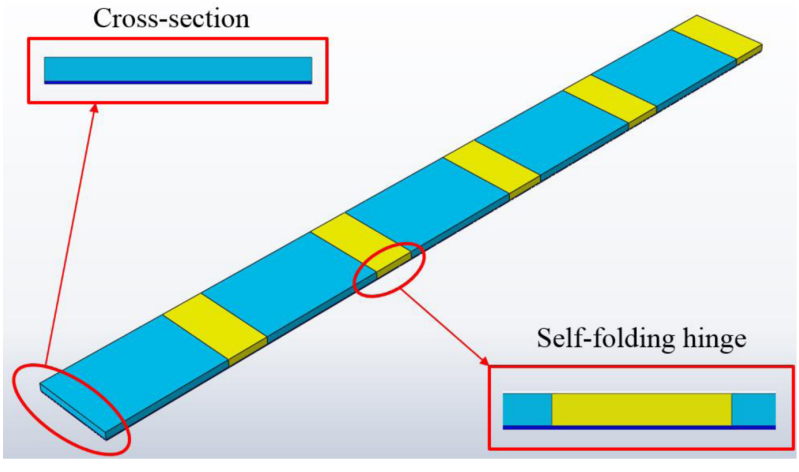

Figure 5. SMP self-folding structure: Plate thickness comprising two layers of blue and dark blue of same SMP material while yellow region as self-folding part.

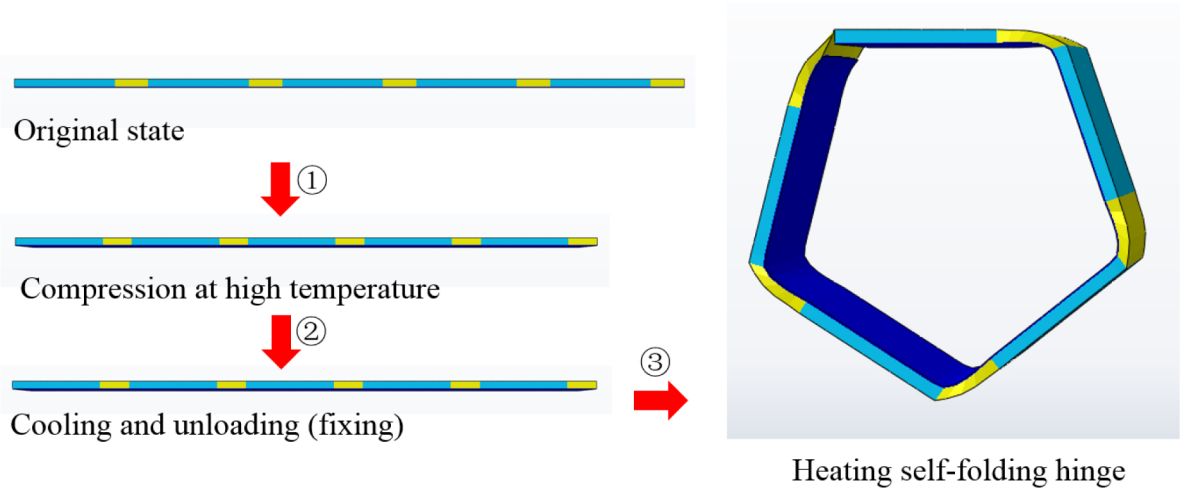

Figure 6. Deformation processes of self-folding structure from 2D to 3D shapes. Arrow 1: plate compressed at high temperature, Arrow 2: plate cooled down and unloaded. Arrow 3: yellow hinge region reheated to form 3D structure.

portions, the two-dimensional plate will fold into a three-dimensional pentagon as illustrated in Figure 6. This simple example demonstrates the potential of SMPs for self-folding applications. Many complex structures can be formed or constructed through the rational design and facilitated via the proposed numerical simulation processes.

6. Concluding remarks

In this paper, we have developed a 3D phase-evolution-based thermomechanical constitutive model for SMPs by extending our previous 1D formulation to enable the analysis of the deformation mechanism at the structural level. The 3D model has been implemented into a finite element package ABAQUS via subroutine UMAT. The proposed theoretical formulation and numerical implementation are validated by the prediction of the shape memory behavior of SMPs under a variety of loading patterns in: (i) tension, (ii) zero-strain and (iii) compression. By comparing results obtained from theoretical calculations, FEM simulations and experiments under the 3 loading conditions, we are confident that the proposed 3D model incorporating FE implementation be able to describe the deformation mechanism of SMP materials reasonably well. FE model as UMAT in ABAQUS is shown to be effective and stable for the study on the shape memory behavior of SMPs. The robustness of the proposed approach is demonstrated through the analyses of 2 complex SMP structures presented in section 5. The tests of the designed hexachiral SMP deployable structure at various stages of deformation mechanism are precisely captured by the numerical solutions conducted in the present study. We also design a self-folding structure comprising a plate with programmed loading and heating regions. The proposed FE solutions show that the designed plate will be morphed into a 3D structure after completing the appropriate programmed processes. The proposed approach accompanied by the finite element implementation will enable researchers to design other functional structures as well as to study the intricate deformation behaviors of various sophisticated SMP structures.

Acknowledgement

The authors are grateful for the support from the National Natural Science Foundation of China through grant numbers 11820101001 and 11572236.

References

[Baghani et al. 2012] M. Baghani, R. Naghdabadi, J. Arghavani, and S. Sohrabpour, "A thermodynamically-consistent 3D constitutive model for shape memory polymers", *Int. J. Plasticity* **35** (2012), 13–30.

[Baghani et al. 2014] M. Baghani, J. Arghavani, and R. Naghdabadi, "A finite deformation constitutive model for shape memory polymers based on Hencky strain", *Mech. Mater.* **73** (2014), 1–10.

[Behl et al. 2010] M. Behl, M. Y. Razzaq, and A. Lendlein, "Multifunctional shape-memory polymers", *Adv. Mater.* **22**:31 (2010), 3388–3410.

[Castano and Flatau 2014] L. M. Castano and A. B. Flatau, "Smart fabric sensors and e-textile technologies: a review", *Smart. Mater. Struct.* **23**:5 (2014), art. id. 053001.

[Chen and Lagoudas 2008a] Y. C. Chen and D. C. Lagoudas, "A constitutive theory for shape memory polymers, I", *J. Mech. Phys. Solids* **56**:5 (2008a), 1752–1765.

[Chen and Lagoudas 2008b] Y. C. Chen and D. C. Lagoudas, "A constitutive theory for shape memory polymers, II", *J. Mech. Phys. Solids* **56**:5 (2008b), 1766–1778.

[Conti et al. 2007] S. Conti, M. Lenz, and M. Rumpf, "Modeling and simulation of magnetic-shape-memory polymer composites", *J. Mech. Phys. Solids* **55** (2007), 1462–1486.

[Diani et al. 2006] J. Diani, Y. Liu, and K. Gall, "Finite strain 3D thermoviscoelastic constitutive model for shape memory polymers", *Poly. Eng. Sci.* **46**:4 (2006), 486–492.

[Diani et al. 2012] J. Diani, P. Gilormini, C. Frédy, and I. Rousseau, "Predicting thermal shape memory of crosslinked polymer networks from linear viscoelasticity", *Int. J. Solids Struct.* **49**:5 (2012), 793–799.

[Eskandari et al. 2018] A. H. Eskandari, M. Baghani, and S. Sohrabpour, "A time-dependent finite element formulation for thick shape memory polymer beams considering shear effects", *Int. J. Appl. Mech.* **10**:4 (2018), art. id. 1850043.

[Fang et al. 2018] C. Q. Fang, J. S. Leng, H. Y. Sun, and J. P. Gu, "A multi-branch thermoviscoelastic model based on fractional derivatives for free recovery behaviors of shape memory polymers", *Mech. Mater.* **120** (2018), 34–42.

[Gilormini and Diani 2012] P. Gilormini and J. Diani, "On modeling shape memory polymers as thermoelastic two-phase composite materials", *C. R. Mécanique* **340**:4-5 (2012), 338–348.

[Gu et al. 2015] J. Gu, H. Sun, and C. Fang, "A phenomenological constitutive model for shape memory polyurethanes", *J. Intel. Mat. Syst. Str.* **26**:5 (2015), 517–526.

[Hager et al. 2015] M. D. Hager, S. Bode, C. Weber, and U. S. Schubert, "Shape memory polymers: past, present and future developments", *Prog. Polym. Sci.* **49** (2015), 3–33.

[He et al. 2015] Y. He, S. Guo, Z. Liu, and K. M. Liew, "Pattern transformation of thermo-responsive shape memory polymer periodic cellular structures", *Int. J. Solids Struct.* **71** (2015), 194–205.

[Hu and Chen 2010] J. L. Hu and S. J. Chen, "A review of actively moving polymers in textile applications", *J. Mater. Chem.* **20**:17 (2010), 3346–3355.

[Hu et al. 2012] J. L. Hu, Y. Zhu, H. H. Huang, and J. Lu, "Recent advances in shape-memory polymers: structure, mechanism, functionality, modeling and applications", *Prog. Polym. Sci.* **37**:12 (2012), 1720–1763.

[Huang et al. 2005] W. Huang, B. Yang, L. An, C. Li, and Y. Chan, "Water-driven programmable polyurethane shape memory polymer: demonstration and mechanism", *Appl. Phys. Lett.* **86** (2005), art. id. 114105.

[Huang et al. 2020] R. Huang, S. J. Zheng, Z. S. Liu, and T. Y. Ng, "Recent advances of the constitutive models of smart materials- hydrogels and shape memory polymers", *Int. J. Appl. Mech.* **12**:2 (2020), art. id. 2050014.

[Lendlein et al. 2005] A. Lendlein, H. Jiang, O. Jünger, and R. Langer, "Light-induced shape-memory polymers", *Nature* **434**:7035 (2005), 879–882.

[Lendlein et al. 2010] A. Lendlein, M. Behl, B. Hiebl, and C. Wischke, "Shape-memory polymers as a technology platform for biomedical applications", *Expert. Rev. Med. Devices* **7**:3 (2010), 0357–379.

[Leng et al. 2009] J. S. Leng, H. B. Lu, Y. J. Liu, W. M. Huang, and S. Y. Du, "Shape-Memory polymers: a class of novel smart materials", *Mrs. Bull.* **34**:11 (2009), 848–855.

[Li and Liu 2018] Y. X. Li and Z. S. Liu, "A novel constitutive model of shape memory polymers combining phase transition and viscoelasticity", *Polymer* **143** (2018), 298–308.

[Li et al. 2015] Y. X. Li, S. S. Guo, Y. H. He, and Z. S. Liu, "A simplified constitutive model for predicting shape memory polymers deformation behavior", *Int. J. Comput. Mater. Sci. Eng.* **4**:1 (2015), art. id. 1550001.

[Li et al. 2017a] Y. X. Li, Y. H. He, and Z. S. Liu, "A viscoelastic constitutive model for shape memory polymers based on multiplicative decompositions of the deformation gradient", *Int. J. Plasticity* **91** (2017a), 300–317.

[Li et al. 2017b] Y. X. Li, J. Y. Hu, and Z. S. Liu, "A constitutive model of shape memory polymers based on glass transition and the concept of frozen strain release rate", *Int. J. Solids Struct.* **124** (2017b), 252–263.

[Li et al. 2018] Y. X. Li, R. X. Liu, and Z. S. Liu, "Study on dynamic behaviors of a shape memory polymer membrane", *Acta. Mech. Solid. Sin.* **31**:5 (2018), 635–651.

[Lin and Chen 1999] J. Lin and L. Chen, "Shape-memorized crosslinked ester-type polyurethane and its mechanical viscoelastic model", *J. Appl. Polym. Sci.* **73**:7 (1999), 1305–1319.

[Liu et al. 2006] Y. Liu, K. Gall, M. L. Dunn, A. R. Greenberg, and J. Diani, "Thermomechanics of shape memory polymers: uniaxial experiments and constitutive modeling", *Int. J. Plasticity* **22**:2 (2006), 279–313.

[Liu et al. 2015] Z. S. Liu, T. William, and T. Y. Ng, "Advances in mechanics of soft materials: a review of large deformation behavior of hydrogels", *Int. J. Appl. Mech.* **7**:5 (2015), art. id. 1530001.

[Liu et al. 2019a] R. X. Liu, Y. X. Li, and Z. S. Liu, "Experimental study on thermo-mechanical behavior of a thermosetting shape memory polymer", *Mech. Time-Depend. Mat.* **23**:3 (2019), 249–266.

[Liu et al. 2019b] R. X. Liu, S. Mcginty, F. S. Cui, X. Y. Luo, and Z. S. Liu, "Modelling and simulation of the expansion of a shape memory polymer stent", *Eng. Comput.* **36**:8 (2019), 2726–2746.

[Lucchesi et al. 2019] M. Lucchesi, B. Pintucchi, and N. Zani, "Orthotropic plane bodies with bounded tensile and compressive strength", *J. Mech. Mater. Struct.* **13**:5 (2019), 691–701.

[Luo and Mather 2013] X. Luo and P. T. Mather, "Shape memory assisted self-healing coating", *ACS Macro. Lett.* **2**:2 (2013), 152–156.

[Moon et al. 2015] S. Moon, F. Cui, and I. J. Rao, "Constitutive modeling of the mechanics associated with triple shape memory polymers", *Int. J. Eng. Sci.* **96** (2015), 86–110.

[Nguyen et al. 2008] T. D. Nguyen, H. J. Qi, F. Castro, and K. N. Long, "A thermoviscoelastic model for amorphous shape memory polymers: incorporating structural and stress relaxation", *J. Mech. Phys. Solids* **56**:9 (2008), 2792–2814.

[Pan and Liu 2018] Z. Z. Pan and Z. S. Liu, "A novel fractional viscoelastic constitutive model for shape memory polymers", *J. Polym. Sci. Pol. Phys.* **56**:16 (2018), 1125–1134.

[Pan et al. 2018] Z. Z. Pan, Y. Zhou, N. Zhang, and Z. S. Liu, "A modified phase-based constitutive model for shape memory polymers", *Polym. Int.* **67**:12 (2018), 1677–1683.

[Pan et al. 2019] Z. Z. Pan, R. Huang, and Z. S. Liu, "Prediction of the thermomechanical behavior of particle reinforced shape memory polymers", *Poly. Comp.* **40**:1 (2019), 353–363.

[Pieczyska et al. 2017] E. A. Pieczyska, M. Staszczak, K. Kowalczyk-Gajewska, M. Maj, K. Golasiński, S. Golba, H. Tobushi, and S. Hayashi, "Experimental and numerical investigation of yielding phenomena in a shape memory polymer subjected to cyclic tension at various strain rate", *Polym. Test.* **60** (2017), 333–342.

[Qi and Dunn 2010] H. J. Qi and M. L. Dunn, "Thermomechanical behavior and modeling approaches", pp. 75–100 in *Shape-memory. polymers and multifunctional composites*, edited by J. Leng and S. Du, CRC Press, 2010.

[Qi et al. 2008] H. J. Qi, T. D. Nguyen, F. Castro, C. M. Yakacki, and R. Shandas, "Finite deformation thermo-mechanical behavior of thermally induced shape memory polymers", *J. Mech. Phys. Solids* **56**:5 (2008), 1730–1751.

[Reese et al. 2010] S. Reese, M. Böl, and D. Christ, "Finite element-based multi-phase modelling of shape memory polymer stents", *Comput. Method. Appl. M* **199**:21-22 (2010), 1276–1286.

[Rossiter et al. 2012] J. Rossiter, F. Scarpa, K. Takashima, and P. Walters, "Design of a deployable structure with shape memory polymers", in *Behavior and mechanics of multifunctional materials and composites* (San Diego, 2012), SPIE **8342**, 2012.

[Shojaei and Li 2014] A. Shojaei and G. Li, "Thermomechanical constitutive modelling of shape memory polymer including continuum functional and mechanical damage effects", *Proc. Roy. Soc. A Math. Phys.* **470**:2170 (2014), art. id. 20140199.

[Shojaei et al. 2013] A. Shojaei, G. Li, and G. Z. Voyiadjis, "Cyclic viscoplastic-viscodamage analysis of shape memory polymers fibers with application to self-healing smart materials", *J. Appl. Mech.* **80**:1 (2013), 819–833.

[Srivastava et al. 2010] V. Srivastava, S. A. Chester, and L. Anand, "Thermally actuated shape-memory polymers: experiments, theory, and numerical simulations", *J. Mech. Phys. Solids* **58**:8 (2010), 1100–1124.

[Tian and Venkatesh 2013] M. Tian and T. A. Venkatesh, "Indentation of shape memory polymers: characterization of thermo-mechanical and shape recovery properties", *Polymer* **54**:4 (2013), 1405–1414.

[Tobushi et al. 1997] H. Tobushi, T. Hashimoto, S. Hayashi, and E. Yamada, "Thermomechanical constitutive modeling in shape memory polymer of polyurethane series", *J. Intel. Mat. Syst. Str.* **8**:8 (1997), 711–718.

[Tolley et al. 2014] M. T. Tolley, S. M. Felton, S. Miyashita, D. Aukes, D. Rus, and R. J. Wood, "Self-folding origami: shape memory composites activated by uniform heating", *Smart. Mat. Struct.* **23**:9 (2014), 094006.

[Valizadeh et al. 2018] I. Valizadeh, P. Steinmann, and A. Javili, "Growth-induced instabilities of an elastic film on a viscoelastic substrate: analytical solution and computational approach via eigenvalue analysis", *J. Mech. Mater. Struct.* **13**:4 (2018), 571–585.

[Volk et al. 2010] B. L. Volk, D. C. Lagoudas, and Y. C. Chen, "Analysis of the finite deformation response of shape memory polymers, II: 1D calibration and numerical implementation of a finite deformation, thermoelastic model", *Smart. Mater. Struct.* **19**:7 (2010), art. id. 075006.

[Yakacki and Gall 2009] C. M. Yakacki and K. Gall, "Shape-memory polymers for biomedical applications", pp. 147–175 in *Shape-Memory polymers*, edited by A. Lendlein, Adv. Polym. Sci. **226**, Springer, 2009.

[Yang and Li 2015] Q. Yang and G. Li, "Temperature and rate dependent thermomechanical modeling of shape memory polymers with physics based phase evolution law", *Int. J. Plasticity* **80** (2015), 168–186.

[Yu et al. 2014] K. Yu, A. J. W. Mcclung, G. P. Tandon, J. W. Baur, and H. J. Qi, "A thermomechanical constitutive model for an epoxy based shape memory polymer and its parameter identifications", *Mech. Time-Depend. Mat.* **18**:2 (2014), 453–474.

[Zheng et al. 2018] S. J. Zheng, Z. Q. Li, and Z. S. Liu, "The fast homogeneous diffusion of hydrogel under different stimuli", *Int. J. Mech. Sci.* **137** (2018), 263–270.

Received 31 Dec 2019. Revised 21 Apr 2020. Accepted 14 May 2020.

YUNXIN LI: liyunxinrrr@stu.xjtu.edu.cn
International Center for Applied Mechanics, State Key Laboratory for Strength and Vibration of Mechanical Structures, Xi'an Jiaotong University, Xi'an, 710049, China

and

Institute of Chemical Materials, CAEP, Mianyang 621999, China

RUOXUAN LIU: liuruoxuan@stu.xjtu.edu.cn
International Center for Applied Mechanics, State Key Laboratory for Strength and Vibration of Mechanical Structures, Xi'an Jiaotong University, Xi'an, 710049, China

ZISHUN LIU: zishunliu@mail.xjtu.edu.cn
International Center for Applied Mechanics, State Key Laboratory for Strength and Vibration of Mechanical Structures, Xi'an Jiaotong University, Xi'an, 710049, China

SOMSAK SWADDIWUDHIPONG: ceesomsa@nus.edu.sg
Department of Civil and Environmental Engineering, National University of Singapore, Singapore 117576, Singapore

JOURNAL OF MECHANICS OF MATERIALS AND STRUCTURES

msp.org/jomms

Founded by Charles R. Steele and Marie-Louise Steele

See msp.org/jomms for submission guidelines.

JoMMS (ISSN 1559-3959) at Mathematical Sciences Publishers, 798 Evans Hall #6840, c/o University of California, Berkeley, CA 94720-3840, is published in 10 issues a year. The subscription price for 2020 is US $660/year for the electronic version, and $830/year (+$60, if shipping outside the US) for print and electronic. Subscriptions, requests for back issues, and changes of address should be sent to MSP.

JoMMS peer-review and production is managed by EditFLOW® from Mathematical Sciences Publishers.

PUBLISHED BY

mathematical sciences publishers

nonprofit scientific publishing

http://msp.org/

Journal of Mechanics of Materials and Structures

Volume 15, No. 3 May 2020

1559-3959(2020)15:3;1-J